Controlling the Early Stages of Pentacene Growth by Supersonic Molecular Beam Deposition

Yu Wu,[1] Tullio Toccoli,[2] Norbert Koch,[3] Erica Iacob,[4] Alessia Pallaoro,[2] Petra Rudolf,[1,*] and Salvatore Iannotta[2]

[1]*Zernike Institute for Advanced Materials, University of Groningen, Nijenborgh 4, NL-9747 AG, Groningen, The Netherlands*
[2]*IFN-CNR, Istituto di Fotonica e Nanotecnologie, Via Sommarive, 18 I-38050 Povo, Trento, Italy*
[3]*Institut für Physik, Humboldt-Universität zu Berlin, Newtonstrasse 15, D-12489 Berlin, Germany*
[4]*IRST—ITC—Physics and Chemistry of Surfaces and Interfaces Division, Via Sommarive, 18 I-38050 Povo, Trento, Italy*

(Received 28 August 2006; published 13 February 2007)

The key role of the pentacene kinetic energy (E_k) in the early stages of growth on SiO_x/Si is demonstrated: islands with smooth borders and increased coalescence differ remarkably from fractal-like thermal growth. Increasing E_k to 6.4 eV, the morphology evolves towards higher density of smaller islands. At higher coverage, coalescence grows with E_k up to a much more uniform, less defected monolayer. The growth, interpreted by the diffusion mediated model, shows the critical nucleus changing from 3 to 2 pentacene for $E_k > 5$–6 eV. Optimal conditions to produce single crystalline films are envisaged.

DOI: 10.1103/PhysRevLett.98.076601 PACS numbers: 72.80.Le, 68.37.Ps, 68.55.Ac, 79.20.Rf

Pentacene (Pen) is one of the most promising candidates for organic electronic applications [1] since it exhibits high hole mobility (up to 5.5 $cm^2/V\,s$) [2] in organic thin film field effect transistors (OTFTs). Nonetheless, the difficulty to determine and to control key properties of the organic layer, such as structure, morphology, and interfaces, is still a major factor limiting electronic properties. In particular, further progress in device development requires highly ordered large size crystals [3], possibly eliminating grain boundaries [1,3]. Recent studies evidenced a viable and promising approach to these questions based on controlling the incident molecules' energy by supersonic molecular beam deposition (SuMBD) [4–6]. Since the film quality is largely determined by the early stages of growth, and since the first few molecular layers are crucial for charge transport in OTFTs [7], we focused on the (sub)monolayer growth on a chemically inert, flat SiO_x/Si surface. Recently, Killampalli *et al.* [8], who studied Pen monolayer deposition on SiO_x/Si by SuMBD at various kinetic energies (1.5–6.7 eV), reported a decreasing adsorption probability for increasing incident kinetic energy (E_k), an island density that does not change appreciably during island growth, and the smallest stable nucleus requiring four molecules. The same critical nucleus was found for thermal evaporation [9,10]. In this Letter, we show that, by tuning the impinging molecules' flux and energy, one can achieve unprecedented control on the condensation nucleus, and on the island density at different growth stages and thus produce films of much better quality. In particular, we demonstrate that, at moderate fluxes, (i) the island density depends markedly on E_k, (ii) the critical nucleus, determined by applying the general scaling function [11] is composed of only two molecules, and (iii) the growth rate increases with E_k. Based on this approach, we established improved conditions for producing highly ordered Pen layers with minimum density of grain boundaries. The different island growth modes are rationalized, as a function of different E_k regimes, in terms of surface diffusivity and its effects on the growth model.

Pen was deposited on a native SiO_x layer [12] prepared by a standard wet chemical oxidation process [10] on silicon. The typical root mean square surface roughness of ~0.5 nm was determined by atomic force microscopy in tapping mode (AFM), by which we also noticed a few bright spots (area density of $\sim 2.5 \times 10^7/cm^2$), presumably due to contamination. All substrates were hydrophilic, with water contact angles of $35 \pm 2°$ determined by the sessile drop method [13]. Pen (Sigma-Aldrich, 99.98%) was purified before use by gradient vacuum sublimation [14]. The SuMBD system was described previously [4]. Samples were prepared by exposure to the supersonic beam ($\approx$ 10 mm diameter), for different times (10, 20, 30, and 50 min), at room temperature. *Ex situ* AFM [15] was systematically carried out by scanning over multiple $10 \times 10\ \mu m^2$ areas at the sample center. The molecular beam was characterized on-line in terms of chemical purity, flux, and energy distribution by combining time of flight (TOF) mass spectrometry and multiphoton ionization spectroscopy. We chose an operating regime where no clustering effects [16] and contaminants were detectable. The typical flux was $\approx 2 \times 10^{11}$ molecules/$(s\,cm^2)$, estimated by cross correlating the TOF spectra at different E_k of the beam with that of a Knudsen Pen source used as a standard.

The four different E_k explored here (3.3, 5.0, 6.4, and 6.7 eV) were achieved by varying the degree of seeding through changing the He carrier gas pressure. The highest E_k achievable in our experimental conditions using He is 6.7 eV.

Figure 1 shows the morphology evolution versus exposure time for two of the E_ks explored. In all cases, as shown by a micrograph at higher resolution in Fig. 2, the shape of islands is uniform (lobular) with smooth borders and hence markedly different from the fractal shapes usually ob-

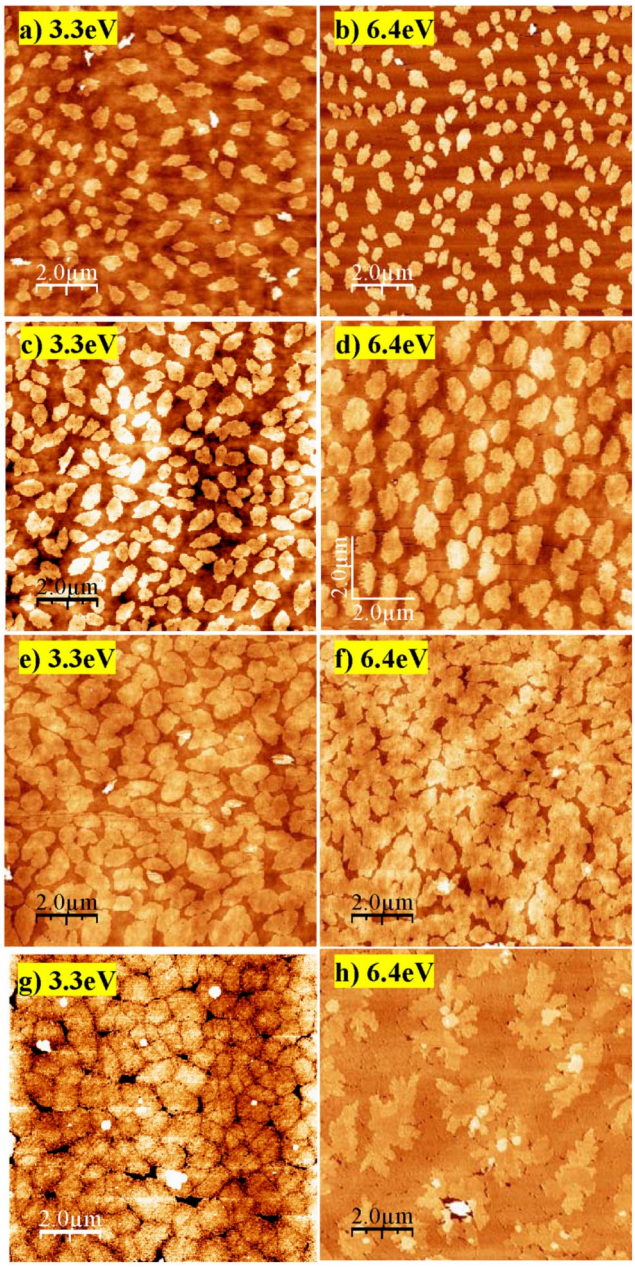

FIG. 1 (color online). AFM micrographs (10×10 μm^2) of pentacene grown by SuMBD at two kinetic energies: $E_k = 3.3$ eV (first column) and $E_k = 6.4$ eV (second column). The evolution of the deposition has been characterized at different exposure times: (a),(b) at 10 min; (c),(d) at 20 min; (e),(f) at 30 min; (g),(h) at 50 min.

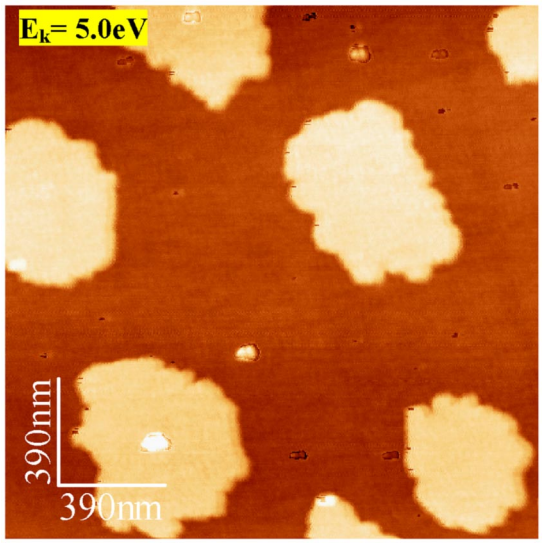

FIG. 2 (color online). High resolution (2.0×2.0 μm^2) AFM micrograph showing the typical island morphology of a film prepared by exposure to a beam of $E_k = 5.0$ eV for 10 min.

served for thermal evaporated layers [17,18]. The top two images in Fig. 1 compare samples produced at an exposure time of 10 min. There are relevant trends that have been systematically observed: at higher kinetic energies ($E_k =$ 5.0 and 6.4 eV) the typical island size shrinks and the island density increases as shown by the molecular island size distributions [Fig. 3(a)]. In particular, samples prepared at 3.3, 5.0, and 6.4 eV exhibit distributions peaking at island sizes of 0.11, 0.10, and 0.09 μm^2, respectively. The broader distribution observed for $E_k = 3.3$ eV is likely related to a more thermal-like growth process, which is expected for this beam as its E_k distribution is closer to thermal. Insight into the growth of Pen from hyperthermal beams can be achieved by considering that it is a diffusion limited process [9,10]. When colliding with the surface, the initial E_k of Pen is converted (partially) into E_k parallel to the surface via a complex mechanism involving inelastic molecule-molecule and molecule-surface energy transfer processes [19–22]. It is reasonable to assume, by extending consolidated growth models [9–11], that molecules with higher E_k diffuse over longer distances before aggregating or being captured by preformed molecular islands. This would result in a more uniformly dispersed pattern of small islands. On the contrary, molecules with lower E_k travel shorter distances and have a lower probability to form new islands by colliding with other freely diffusing molecules at empty sites. A quantitative assessment was achieved by determining the critical nucleus i ($i + 1 =$ number of molecules forming a stable nucleus), based on the general scaling function $f_i(u) = C_i u^i e^{-i a_i u^{1/a_i}}$ introduced by Amar and Family [11], extended to Pen growth by Ruiz *et al.* [9], and reproposed by Tejima *et al.* and Stadlober *et al.* [23,24]. C_i and a_i are constants determined by hypergeometrical equations for $i = 0, \ldots, 3$ that assure normalization and proper asymptotic behavior of $f_i(u)$. Figure 3(b) compares the normalized island size distributions of films grown at $E_k = 3.3$ and 6.4 eV with the predictions of the general scaling model calculated for $i =$ 1, 2, and 3. For the highest E_k, we systematically observed a much better agreement for $i = 2$, as confirmed by a χ^2 criterion. At about $E_k \leq 5.5$–6.0 eV the experimental dis-

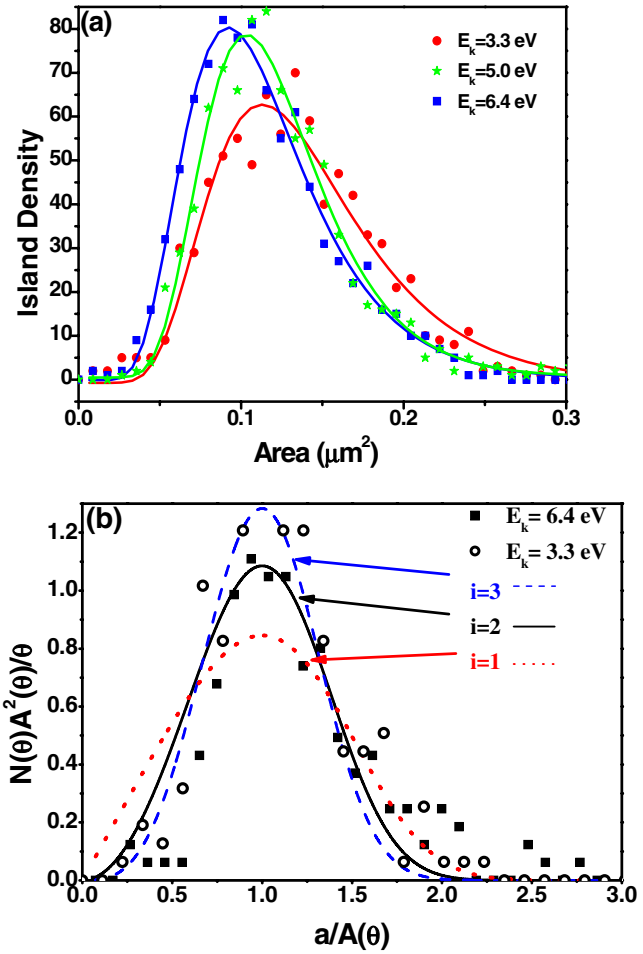

FIG. 3 (color online). (a) Typical molecular island size distributions of films grown, by 10 min exposure, to the supersonic beam operated at three pentacene different E_k: 3.3, 5.0, and 6.4 eV. (b) The properly normalized island distributions of films formed at $E_k = 6.4$ eV (■) and $E_k = 3.3$ eV (○) indicate different critical island sizes, respectively, $i = 2$ and $i = 3$, in the framework of the scaling function predictions reported in the plot as dashed line ($i = 3$), continuous line ($i = 2$), and dotted line ($i = 1$), respectively, (see text).

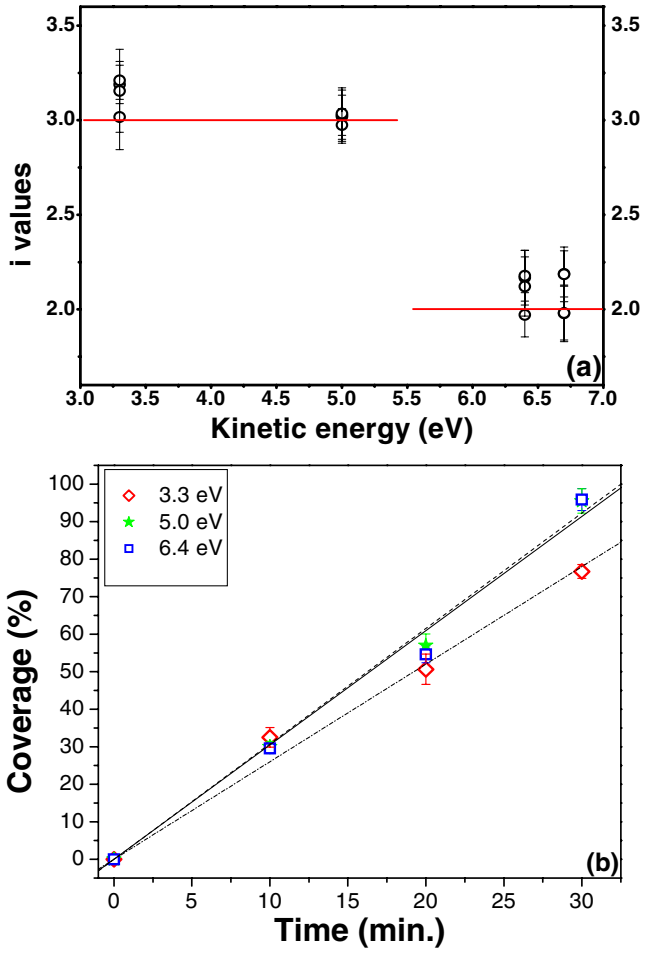

FIG. 4 (color online). (a) Critical island sizes extracted from the experimental island distributions as a function of the E_k of the pentacene molecules, for 10 min deposition time. The lines for $i = 2$ and $i = 3$ are shown as a reference to guide the eye. A transition between two different growth regimes is observed at about 5.5–6.0 eV. (b) Surface coverage evolution as a function of exposure time for pentacene growth on SiO_x/Si. Slightly different rates are observed for low and high pentacene E_k.

tribution is better reproduced by the $i = 3$ distribution, as previously reported for thermally deposited films on similar substrates [9,23,24]. By analyzing different sets of data by best fitting procedures, we corroborated the critical nucleus decrease from 3 to 2 over a threshold of E_k as shown in Fig. 4(a). The diffusion growth model confirms the important role played by E_k in the diffusion mediated processes regulating island formation and growth. An understanding of the mechanism by which a smaller critical nucleus can generate a higher final correlation length can be gained by considering that it implies a much higher density of nucleation sites, which proportionally reduces the island-island distance. Since the growth is diffusion mediated, such higher density shifts the onset of the island-island coalescence process to a much earlier stage of island ripening. The final outcome is that smaller and more mobile islands can merge easier in a crystalline film with reduced grain boundaries and hence a higher surface correlation length.

As evidenced in Figs. 1(c) and 1(d) after 20 min exposure the samples prepared at the highest E_k show island coalescence, not observed for the lower E_k. It appears that for samples prepared at 3.3 eV the competition between growth of preformed islands and nucleation of new islands is still important, as indicated by the increase of island density. This process continues as the exposure time increases [Figs. 1(e) and 1(f)]. At this stage one observes a higher coverage for the highest E_k at the same flux, as also confirmed by x-ray photoelectron spectroscopy measurements on the same samples. Already only 30 min of

exposure to the 6.4 eV beam yields an almost complete monolayer.

Figures 1(g) and 1(h) present the films formed after 50 min exposure, where second layer islands are seen on top of the completed monolayer for the sample prepared at 6.4 eV. The latter shows a much better monolayer quality with a much lower defect density, quasicompletely coalesced islands, a flatter surface, and sharper island edges (where visible). For all samples the monolayer is (1.5 ± 0.2) nm thick, and the formation of a second molecular layer is observed only after the (near) completion of the first. This indicates that molecules landing on top of a molecular island have enough energy to overcome the edge barrier [10] and to move down onto the bare substrate. The samples prepared at 3.3 eV show more grain boundaries with a smaller average molecular island size ($\sim 0.5\ \mu m^2$). It appears that the coverage, and hence growth rate, increases with E_k, with a rate difference that becomes more evident at larger coverage [Fig. 4(b)]. This can be understood within the diffusion mediated growth model considering the higher corrugation of the molecular island surface compared to the bare substrate. Seemingly the higher E_k becomes crucial when the probability of landing on top of molecular islands is larger and both the increase in diffusion length and the need to overcome the barrier at the island edges determine the growth regime.

When comparing our findings to those of Killampalli *et al.* [8], the differences in the coverage dependence, the observed morphologies, and the critical nucleus are quite striking. Our results demonstrate that dissimilar growth regimes can be achieved in SuMBD by tuning E_k and flux (the growth rates reported here are about a factor 50 lower than in [8]).

In conclusion, we have highlighted the key role of molecular kinetic energy in SuMBD, which we successfully used to control the early stage growth of Pen layers. By increasing E_k we could decrease the area density of structural defects in the monolayer, a critical step in achieving optimal growth conditions for organic films of unprecedented crystalline quality. We interpreted the impact of E_k in terms of the diffusion mediated model and found that the critical nucleus reduces from $i = 3$ (typical for thermal sublimation) to $i = 2$ for $E_k > 5$–6 eV. A next step will be to investigate how the growth by SuMBD is influenced by different surface properties, such as the hydrophilic-hydrophobic character of the substrates.

We gratefully acknowledge technical support by C. Corradi, M. Mazzola, and N. Tombros, and discussions with R. Verucchi, L. Aversa, I. Arfaoui, M. Lubomska, M. Nardi, and F. Siviero. We thank O. D. Jurchescu (Pen purification) and A. Heeres and E. Maccallini (XPS) as well as the Physics of Nanodevices group of the Zernike Institute for Advanced Materials, University of Groningen, for use of the AFM. This work was financially supported by Italian Ministry of Research FIRB projects SQUARE (RBNE01Y8C3_007) and Synergy; by the FUR—Provincia Autonoma di Trento—projects RASO2 and NanoCOSHy, by the Dutch Foundation for Fundamental Research on Matter, and by the Breedtestrategie program of the University of Groningen. N. K. acknowledges financial support by the Emmy Noether-Program (DFG).

*Corresponding author.
Electronic address: p.rudolf@rug.nl

[1] C. D. Dimitrakopoulos and P. R. L. Malenfant, Adv. Mater. **14**, 99 (2002).
[2] S. Lee *et al.*, Appl. Phys. Lett. **88**, 162109 (2006).
[3] G. Horowitz, J. Mater. Res. **19**, 1946 (2004).
[4] S. Iannotta and T. Toccoli, J. Polym. Sci., B Polym. Phys. **41**, 2501 (2003).
[5] L. Casalis *et al.*, Phys. Rev. Lett. **90**, 206101 (2003).
[6] F. De Angelis *et al.*, Synth. Met. **146**, 291 (2004).
[7] F. Dinelli *et al.*, Phys. Rev. Lett. **92**, 116802 (2004).
[8] A. S. Killampalli, T. W. Schroeder, and J. R. Engstrom, Appl. Phys. Lett. **87**, 033110 (2005).
[9] R. Ruiz *et al.*, Phys. Rev. Lett. **91**, 136102 (2003).
[10] R. Ruiz *et al.*, Chem. Mater. **16**, 4497 (2004).
[11] J. G. Amar and F. Family, Phys. Rev. Lett. **74**, 2066 (1995).
[12] The thickness of the SiO_x layer was determined from ellipsometry measurements (Imaging Ellipsometry, Nanofilm Technology GmbH, Germany).
[13] A. W. Neumann and R. J. Good, in *Surface and Colloid Science*, edited by R. J. Good and R. R. Stromberg (Plenum, New York, 1979), Vol. 11.
[14] O. D. Jurchescu, J. Baas, and T. M. Palstra, Appl. Phys. Lett. **84**, 3061 (2004).
[15] The AFM images were acquired with a multimode scanning probe microscope, Digital Instruments, Veeco Metrology Group, U.S. The detailed analysis of AFM data was carried by WSXM (version 7.71, Nanotec Electronica S.L.) software.
[16] P. Milani and S. Iannotta, *Cluster Beam Synthesis of Nano-Structured Materials* (Springer-Verlag, Berlin, 1999).
[17] S. Pratontep *et al.*, Phys. Rev. B **72**, 085211 (2005).
[18] R. Ruiz *et al.*, Phys. Rev. B **67**, 125406 (2003).
[19] C. T. Rettner *et al.*, J. Phys. Chem. **100**, 13 021 (1996).
[20] C. T. Reeves *et al.*, J. Chem. Phys. **111**, 7567 (1999).
[21] F. O. Goodman and H. Y. Wachman, *Dynamics of Gas Surface Scattering* (Academic, New York, 1976).
[22] S. Iannotta *et al.*, Chem. Phys. **194**, 133 (1995).
[23] M. Tejima *et al.*, Appl. Phys. Lett. **85**, 3746 (2004).
[24] B. Stadlober *et al.*, Phys. Rev. B **74**, 165302 (2006).